Hindawi
Shock and Vibration
Volume 2021, Article ID 8648000, 17 pages
https://doi.org/10.1155/2021/8648000

*Research Article*

# An Analytical Solution for Seismic Interaction between Urban River-Canyon Topography and Nearby Buildings

**Liguo Jin**,[1,2,3] **Xujin Liu**,[2] **Zhenghua Zhou**,[2,3] **and Su Chen**[4]

[1]*Institute of Geotechnical Engineering, Nanjing Tech University, Nanjing 210009, China*
[2]*School of Transportation Engineering, Nanjing Tech University, Nanjing 210009, China*
[3]*Institute of Engineering Mechanics, Nanjing Tech University, Nanjing 210009, China*
[4]*Key Laboratory of Urban Security and Disaster Engineering of Ministry of Education, Beijing University of Technology, Beijing 100124, China*

Correspondence should be addressed to Su Chen; chensuchina@126.com

Received 11 May 2021; Revised 25 June 2021; Accepted 23 August 2021; Published 8 September 2021

Academic Editor: Zengshun Chen



The interaction between urban river-canyon topography and the river-side building is investigated by using a whole analytic model of a semicircle river-canyon and a shear wall supported by a semicircle rigid foundation embedded in a homogenous half-space. The closed-form analytical solution for system response is presented based on the wave function expansion method. The analysis focuses on the effects of the canyon-building interaction on system response. The strength of the interaction between the river-canyon topography and the building changes periodically as the distance between the canyon and the structure increases, leading to the interaction having beneficial or harmful effects on the building's seismic response. The foundation peak response of the building can be amplified by about 10%, and the peak of the building relative response can be amplified by about 40%. The distribution of canyon-structure spacing with strong or weak interaction is closely related to the dynamic characteristics of the building and the incident angle of the wave. When designing buildings along the river, the building and canyon should be analyzed as a whole model to determine whether the location of the building is in a position with strong interaction with the river-canyon. The model in this paper may be useful for obtaining insight into the effects of canyon-structure interaction and interpreting the observed response in buildings and seismic response estimation in general.

## 1. Introduction

This paper investigates the interaction between urban river-canyon and river-side building by using an analytical model. The work in this article is an extension of Trifunac's researches on the seismic response analysis of a single building [1] and a single canyon [2]. The problem studied in this paper involves the seismic interaction between urban local irregular topography and nearby buildings, which is currently termed as site-city interaction [3–5].

In the past, the amplification effect of canyon topography on ground motions received widespread attention [6–24]. However, scholars considered this amplification effect of canyon topography on building responses only through studying the ground motion characteristics of canyon sites rather than directly seeing the canyon and the nearby buildings as a whole model to study the interaction. Actually, when a strong earthquake occurs, seismic waves scatter on the canyon boundary and the surface of the building foundation. Their scattering wave fields will couple with each other, forming the complex canyon-structure interaction system. Therefore, the ground motion characteristics of the canyon site and the building seismic response are no longer determined only by the seismic response characteristics of the canyon site. The correct results may not be obtained if only the canyon topography and the surrounding soil are taken out for analysis. It is reasonable to analyze the river-canyon, the soil, and the buildings along the river as a whole model.

This paper proposes a two-dimensional overall analytical model of the interaction between the canyon topography and

the buildings along the river. This model consists of a 2D infinite long shear wall supported by a rigid foundation along a river-canyon embedded in a homogenous half-space, subjected by incident SH wave. The closed-form analytical solution of the canyon-structure interaction system response is obtained. The closed-form analytical solution is further used to reveal the interaction mechanism of the canyon-structure system.

In the next section, the methodology is presented, followed by the verification through comparison with the published results. Then, the results in the frequency domain are presented and the anti-plane building response and canyon motion are discussed. Finally, the main findings and the conclusions are summarized.

## 2. Methodology

*2.1. Analytical Model.* The dynamic interaction model of canyon-structure, as shown in Figure 1, consists of a river-canyon and a shear wall, infinitely long in the $y$-direction, standing on a rigid foundation embedded in a half-space. With the points of $o_1$ and $o_2$ as the origin, there are two sets of coordinate systems. The rectangular coordinates and the corresponding cylindrical coordinates are drawn. The $y$-axis of the rectangular coordinate system is perpendicular to the paper (points to the reader). The river-canyon and the rigid foundations are semicircular with the centers at points of $o_1$ and $o_2$, respectively, and the radii are $a$ and $b$, respectively. The half-space and the shear wall are assumed to be linearly elastic, uniform, and isotropic, and the boundary between the rigid foundation and the half-space is assumed to be tightly connected. The half-space is marked with shear modulus $\mu$, shear wave velocity $\beta$, and mass density $\rho$. Within the unit length along the $y$-axis, the mass of the rigid foundation is $M_0$. The shear wall has shear wave velocity $\beta_b$, height $H$, undamped natural frequency $\omega_b$, and mass $M_b$ per unit length in the $y$-direction. The distance between the canyon center $o_1$ and the foundation center $o_2$ is $D$. The excitation is an incident plane SH wave with circular frequency $\omega$, incidence angle $\gamma$ measured from the vertical $z$-axis, and unit amplitude.

To illustrate the canyon deformation, Figure 2 shows 5 observation points on the canyon which are chosen to compute their motions. These are point 1 ($r_1 = a$, $\theta_1 = -\pi/2$), point 2 ($r_1 = a$, $\theta_1 = -\pi/4$), point 3 ($r_1 = a$, $\theta_1 = 0$), point 4 ($r_1 = a$, $\theta_1 = -\pi/4$), and point 5 ($r_1 = a$, $\theta_1 = -\pi/2$), with point 3 being at the bottom of the canyon.

*2.2. Governing Equations and Solution.* In the local coordinate system ($x_1$-$y_1$-$z_1$) of the canyon, the motion in the half-space along the $y$-axis direction caused by the incident SH wave can be written as

$$v^i = \exp\left[i\omega\left(t - \frac{x_1}{c_x} + \frac{z_1}{c_z}\right)\right], \tag{1}$$

where $c_x$ and $c_z$ represent the phase velocities of waves along the $x$- and $z$-axes, respectively

$$c_x = \frac{\beta}{\sin\gamma}, \qquad c_z = \frac{\beta}{\cos\gamma}. \tag{2}$$

The free-field motion consists of the incident wave $v^i$ and the reflected wave $v^r$ on the surface of half-space.

$$v^{i+r} = v^i + v^r = 2\exp\left[i\omega\left(t - \frac{x_1}{c_x}\right)\right]\cos\left(\frac{\omega z_1}{c_z}\right). \tag{3}$$

In the area near the canyon and foundation, the wave field is composed of three parts, which are (A) the free-field motion expressed by equation (3), (B) the scattering field of waves caused by the canyon boundary at $r_1 = a$, and (C) the scattering field generated by the rigid foundation boundary at $r_2 = b$. Since (B) and (C) represent the wavefield radiating outward in the half-space, the form of their final solution must be the same. The time factor $\exp(i\omega t)$ is omitted in the following solutions.

All the wave motions $v^{i+r}$, $v_1^R$, and $v_2^R$ must satisfy the wave differential equation

$$\frac{\partial^2 v}{\partial r^2} + \frac{1}{r}\frac{\partial v}{\partial r} + \frac{1}{r^2}\frac{\partial^2 v}{\partial \theta^2} = \frac{1}{\beta^2}\frac{\partial^2 v}{\partial t^2}, \tag{4}$$

where $v$ stands for the three wave motions $v^{i+r}$, $v_1^R$, and $v_2^R$, respectively. The three wave motions should satisfy the boundary conditions given by

$$\sigma_{\theta y} = \frac{\mu}{r_1}\frac{\partial\left(v^{i+r} + v_1^R + v_2^R\right)}{\partial\theta_1} = 0, \quad \text{at } \theta_1 = \pm\frac{\pi}{2} \text{ and } r_1 > a, \tag{5}$$

$$\sigma_{ry} = \mu\frac{\partial\left(v^{i+r} + v_1^R + v_2^R\right)}{\partial r_1} = 0, \quad \text{at } |\theta_1| < \frac{\pi}{2} \text{ and } r_1 = a, \tag{6}$$

$$v^{i+r} + v_1^R + v_2^R = \Delta, \quad \text{at } r_2 = b. \tag{7}$$

In the local coordinate system ($r_1$-$o_1$-$\theta_1$) of the canyon, the free-field motion $v^{i+r}$ in the half-space along the $y$-axis caused by the incident SH wave can be expanded into Fourier-Bessel series as

$$v^{i+r} = 2J_0(kr_1) + 4\sum_{n=1}^{\infty}(-1)^n J_{2n}(kr_1)\cdot\cos(2n\gamma)\cdot\cos(2n\theta_1) - 4i\sum_{n=0}^{\infty}(-1)^n J_{2n+1}(kr_1)\cdot\sin(2n+1)\gamma\cdot\sin(2n+1)\theta_1. \tag{8}$$

Similarly, in the local coordinate system ($r_2$-$o_2$-$\theta_2$), the free-field motion $v^{1+r}$ can also be expanded into

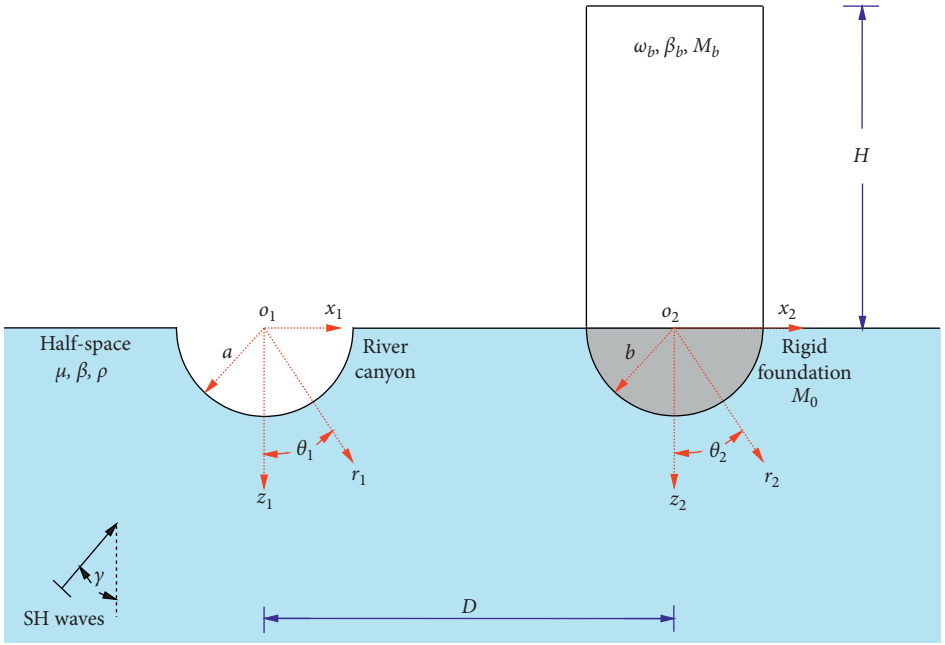


Figure 1: The model of dynamic canyon-structure interaction with an out-of-plane infinite long shear wall standing on a rigid foundation along a river-canyon.

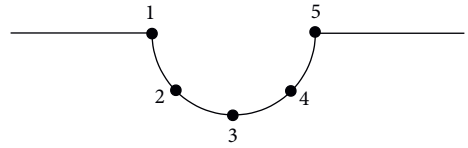


Figure 2: Observation points 1, 2, 3, 4, and 5 of the semicircular river-canyon. Points 1 and 5 are the two corners of the canyon. Point 3 is at the bottom of the canyon.

$$v^{i+r} = \exp(-ikD \cdot \sin\gamma) \cdot \left\{ \begin{array}{l} 2J_0(kr_2) + 4\sum_{n=1}^{\infty} (-1)^n J_{2n}(kr_2) \cdot \cos(2n\gamma) \cdot \cos(2n\theta_2) \\ -4i\sum_{n=0}^{\infty} (-1)^n J_{2n+1}(kr_2) \cdot \sin(2n+1)\gamma \cdot \sin(2n+1)\theta_2 \end{array} \right\}. \tag{9}$$

Here, $J_n(x)$ is the Bessel function of the first kind with argument $x$ and order $n$, and $k = \omega/\beta$.

The scattering wave motions near the canyon and the two foundations can be written as

$$v_1^R = \sum_{n=0}^{\infty} \left[ A_n H_{2n}^{(2)}(kr_1) \cdot \cos(2n\theta_1) + B_n H_{2n+1}^{(2)}(kr_1) \cdot \sin(2n+1)\theta_1 \right], \tag{10}$$

$$v_2^R = \sum_{n=0}^{\infty} \left[ C_n H_{2n}^{(2)}(kr_2) \cdot \cos(2n\theta_2) + D_n H_{2n+1}^{(2)}(kr_2) \cdot \sin(2n+1)\theta_2 \right]. \tag{11}$$

Here, $v_1^R$ and $v_2^R$ are the scattering wave motions from the canyon and the foundation, respectively, and $H_n^{(2)}(x)$ is the Hankel function of the second kind with argument $x$ and order $n$.

Equations (8)–(11) can be proved to satisfy equation (4) and the boundary condition equation (5). $A_n$, $B_n$, $C_n$, and $D_n$ are the unknown complex coefficients that should be determined by the boundary conditions equations (6) and (7).

$\Delta$ is the effective input motion of the rigid foundation to the superstructure.

Because equations (10) and (11) are expressed in different local cylindrical coordinate systems, equations (10) and (11) should be transformed between any two local cylindrical coordinate systems as shown in Figure 1. Based on Graf's Addition Theorem [25, 26], equations (10) and (11) can be transformed between any two cylindrical coordinate systems in Figure 1. The details of the derivation of the coordinate transformation formula are omitted.

Putting equations (8), (10), and (11) into equation (6), we obtain the following equations:

$$A_0 k H_1^{(2)}(ka) + G_{3,n} \cdot \frac{\varepsilon_0}{2} \cdot k \cdot J_1(ka) = -2k \cdot J_1(ka) \quad (m = 0), \tag{12}$$

$$\begin{aligned} &A_m \left[ \frac{2m}{a} H_{2m}^{(2)}(ka) - k \cdot H_{2m+1}^{(2)}(ka) \right] + G_{3,n} \cdot \frac{\varepsilon_{2m}}{2} \cdot \left[ \frac{2m}{a} J_{2m}(ka) - k \cdot J_{2m+1}(ka) \right] \\ &\quad = -4 \cdot (-1)^m \left[ \frac{2m}{a} J_{2m}(ka) - k \cdot J_{2m+1}(ka) \right] \cdot \cos(2m\gamma) \quad (m = 1, 2, 3, \ldots), \end{aligned} \tag{13}$$

$$\begin{aligned} &B_m \left[ \frac{2m+1}{a} H_{2m+1}^{(2)}(ka) - k H_{2m+2}^{(2)}(ka) \right] + G_{4,n} \cdot \frac{\varepsilon_{2m+1}}{2} \left[ \frac{2m+1}{a} J_{2m+1}(ka) - k J_{2m+2}(ka) \right] \\ &\quad = 4i \cdot (-1)^m \left[ \frac{2m+1}{a} J_{2m+1}(ka) - k \cdot J_{2m+2}(ka) \right] \cdot \sin(2m+1)\gamma \quad (m = 0, 1, 2, 3, \ldots). \end{aligned} \tag{14}$$

Submitting equations (9)– (11) into equation (7), we obtain the following equations:

$$C_0 H_0^{(2)}(kb) + G_{1,n} \cdot \frac{\varepsilon_0}{2} \cdot J_0(kb) - \Delta = -2 \exp(-ik\, D \cdot \sin\gamma) \cdot J_0(kb) \quad (m = 0), \tag{15}$$

$$C_m H_{2m}^{(2)}(kb) + G_{1,n} \cdot \frac{\varepsilon_{2m}}{2} \cdot J_{2m}(kb) = -4 \exp(-ik\, D \cdot \sin\gamma) \cdot (-1)^m \cdot J_{2m}(kb) \cdot \cos(2m\gamma) \quad (m = 1, 2, 3, \ldots), \tag{16}$$

$$D_m H_{2m+1}^{(2)}(kb) - G_{2,n} \cdot \frac{\varepsilon_{2m+1}}{2} \cdot J_{2m+1}(kb) = 4i \cdot \exp(-ik\, D \cdot \sin\gamma) \cdot (-1)^m \cdot J_{2m+1}(kb) \cdot \sin(2m+1)\gamma \quad (m = 0, 1, 2, 3, \ldots). \tag{17}$$

Here, $G_{1,n} \sim G_{4,n}$ are presented as follows:

$$G_{1,n} = \sum_{n=0}^{+\infty} \left[ A_n \cdot F1H_{m,2n}^{+}(k\,D) - B_n \cdot F2H_{m,2n+1}^{-}(k\,D) \right], \tag{18a}$$

$$G_{2,n} = \sum_{n=0}^{+\infty} \left[ A_n \cdot F2H_{m,2n}^{+}(k\,D) + B_n \cdot F1H_{m,2n+1}^{-}(k\,D) \right], \tag{18b}$$

$$G_{3,n} = \sum_{n=0}^{+\infty} \left[ C_n \cdot F1H_{m,2n}^{+}(k\,D) + D_n \cdot F2H_{m,2n+1}^{-}(k\,D) \right], \tag{18c}$$

$$G_{4,n} = \sum_{n=0}^{+\infty} \left[ C_n \cdot F2H_{m,2n}^{+}(k\,D) + D_n \cdot F1H_{m,2n+1}^{-}(k\,D) \right], \tag{18d}$$

$$\begin{cases} F1C_{m,n}^{\pm}(kD) = C_{m+n}(kD)\cdot \cos\dfrac{m-n}{2}\pi \pm (-1)^m \cdot C_{n-m}(kD)\cdot \cos\dfrac{m+n}{2}\pi, \\ F2C_{m,n}^{\pm}(kD) = C_{m+n}(kD)\cdot \sin\dfrac{m-n}{2}\pi \pm (-1)^m \cdot C_{n-m}(kD)\cdot \sin\dfrac{m+n}{2}\pi, \\ \varepsilon_m = \begin{cases} 1, & m = 0, \\ 2, & m = 1,2,3,\ldots, \end{cases} \end{cases} \tag{18e}$$

where, in equation (18e), replacing $C$ with $H$ stands for coordinate transformation for Hankel function.

The foundation effective input motion $\Delta$ can be determined by the dynamic equilibrium equation of the rigid foundation.

$$-\omega^2 M_0 \Delta = -\left(f_z^s + f_z^b\right), \tag{19}$$

where, $f_z^b$, the action per unit length of the shear wall on the foundation, is given by equation (20). $f_z^s$ is the action of the soil on the foundations, given by equation (21).

$$f_z^b = -\omega^2 M_b \frac{\tan k_b H}{k_b H}\Delta, \quad k_b = \frac{\omega}{\beta_b}, \tag{20}$$

$$\begin{aligned} f_z^s &= -b\int_{-(\pi/2)}^{\pi/2} \sigma_{rz}|_{r_2=a}\mathrm{d}\theta_2 \\ &= \mu b\pi\left[\exp(-ikD\cdot \sin\gamma)\cdot 2J_1(kb)\right. \\ &\quad \left. + C_0\cdot kH_1^{(2)}(kb) + G_{1,n}\cdot kJ_1(kb)\cdot\frac{\varepsilon_0}{2}\right]. \end{aligned} \tag{21}$$

By submitting equations (20) and (21) into equation (19), it can be shown that

$$\begin{aligned} &C_0\cdot \mu b\pi k H_1^{(2)}(kb) + G_{1,n}\cdot \mu b\pi k\cdot J_1(kb)\cdot\frac{\varepsilon_0}{2} \\ &-\omega^2\left(M_0 + M_b\frac{\tan k_b H}{k_b H}\right)\Delta = \\ &-2\mu b\pi k\cdot \exp(-ikD\cdot \sin\gamma)\cdot J_1(kb) \quad (m = 1,2,3,\ldots). \end{aligned} \tag{22}$$

The unknown complex coefficients $A_n$, $B_n$, $C_n$, $D_n$, and $\Delta$ are determined by solving the linear equations (12)–(17) and (22) together, and the closed-form analytical solution of the problem can be obtained. Particularly, the relative responses of the shear wall to the foundation can be expressed as

$$\Delta^b = \Delta\left(\frac{1}{\cos k_b H} - 1\right). \tag{23}$$

To compare with the published results, $\Delta$ and $\Delta^b$ are normalized by the surface displacement amplitude of free-field ground motion as

$$\begin{aligned} \overline{\Delta} &= \frac{\Delta}{\left|v^{i+r}\right|}, \\ \overline{\Delta}^b &= \frac{\Delta^b}{\left|v^{i+r}\right|}. \end{aligned} \tag{24}$$

*2.3. Impedance Function of the Rigid Foundation.* According to the definition of impedance function, the foundation has unit displacement response ($\Delta = 1$) at this time. The wave field in the half-space only has canyon scattering field $v_1^{R*}$ and foundation scattering field $v_2^{R*}$, but does not include free-field wave motion,

$$\begin{aligned} v_1^{R*} &= \sum_{n=0}^{\infty}\left[A_n^* H_{2n}^{(2)}(kr_1)\cdot \cos(2n\theta_1) + B_n^* H_{2n+1}^{(2)}(kr_1)\cdot \sin(2n+1)\theta_1\right], \\ v_2^{R*} &= \sum_{n=0}^{\infty}\left[C_n^* H_{2n}^{(2)}(kr_2)\cdot \cos(2n\theta_2) + D_n^* H_{2n+1}^{(2)}(kr_2)\cdot \sin(2n+1)\theta_2\right]. \end{aligned} \tag{25}$$

The boundary conditions are

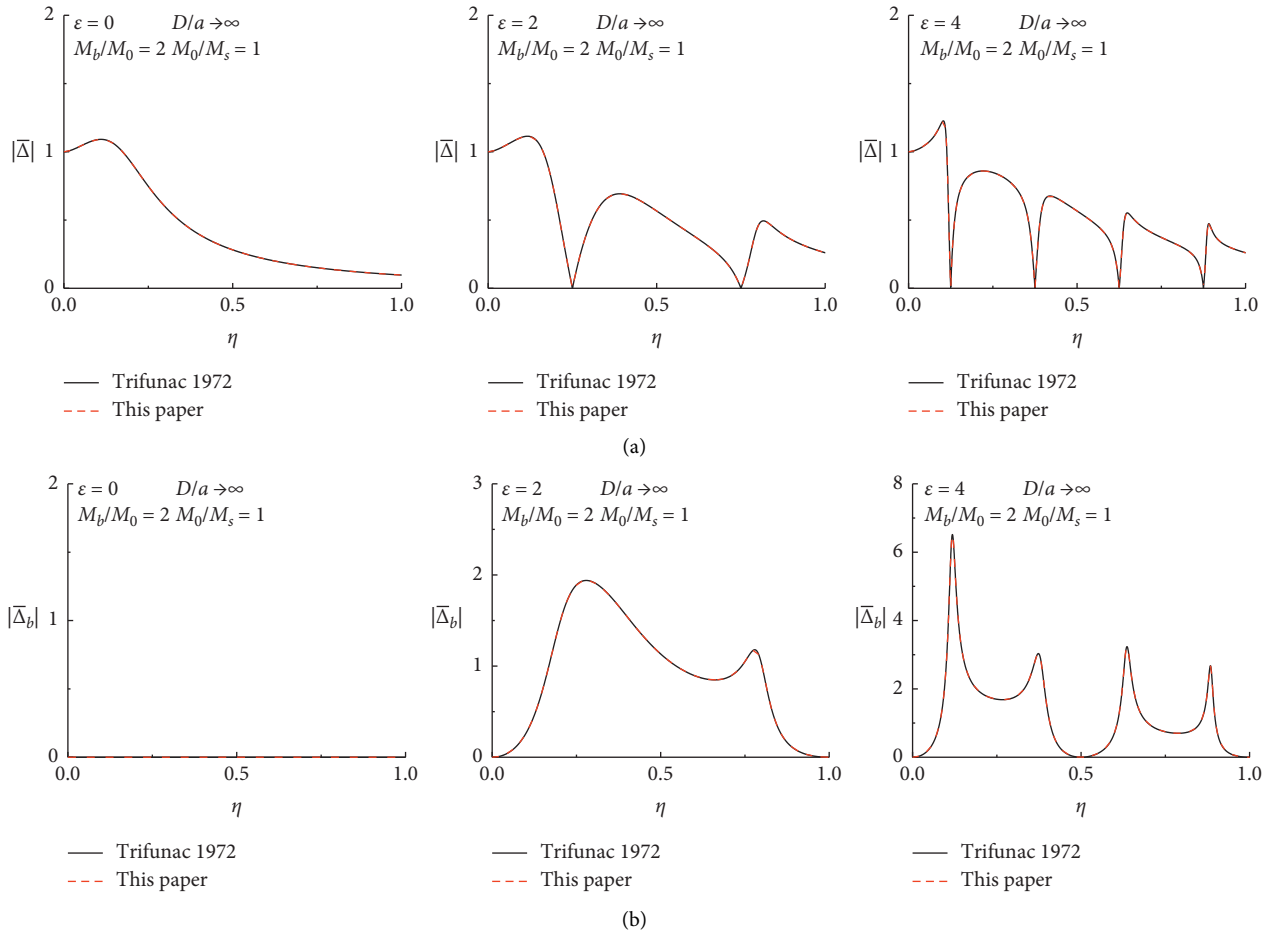


Figure 3: Comparison with the published results of single building [1] for foundation responses (a) and shear wall relative responses (b).

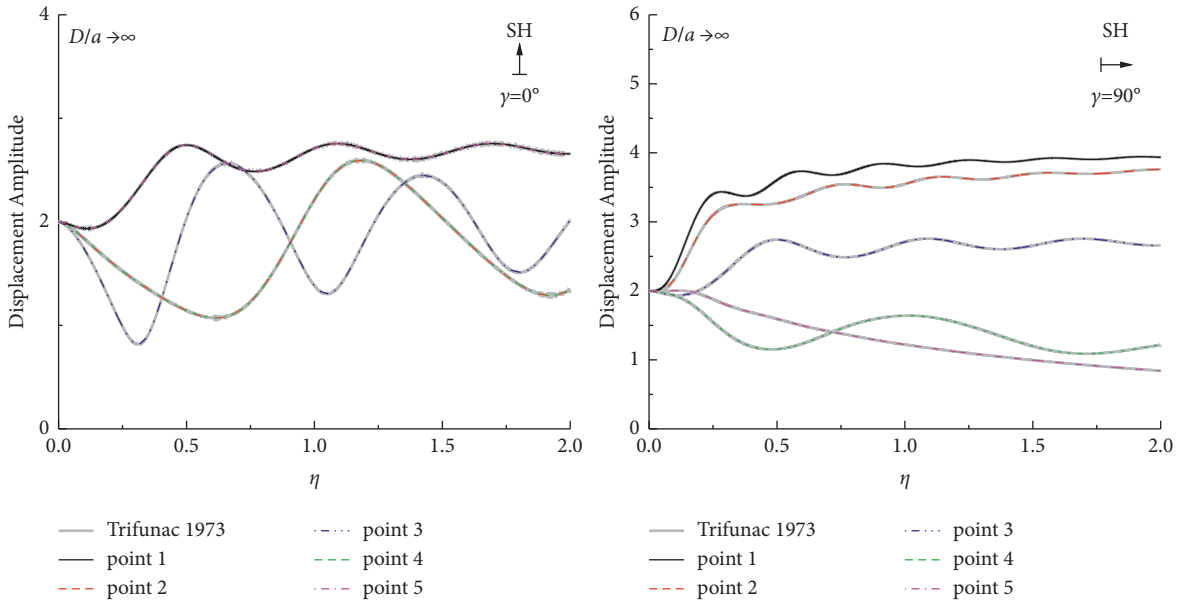


Figure 4: Comparison with the published results of single canyon [2] for typical spectral amplification.

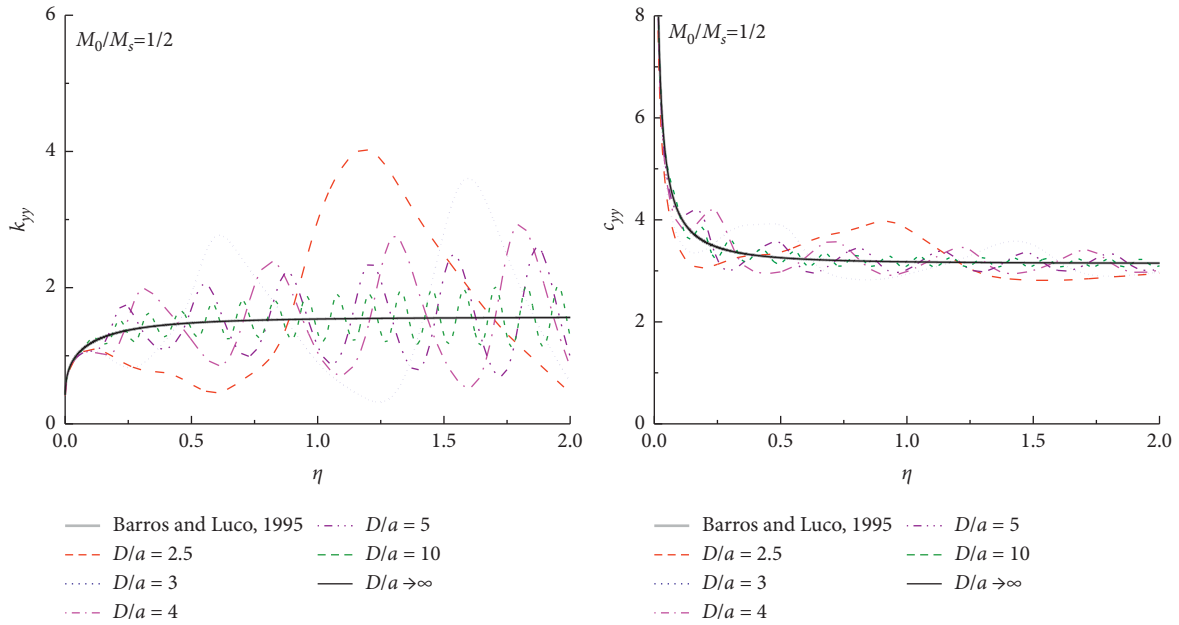


FIGURE 5: Comparison with the impedance function of the single rigid foundation [29]. (a) The stiffness coefficient $k_{yy}$. (b) The damping coefficient $c_{yy}$. The different color line corresponds to the different canyon-building spacing $D/a$.

$$\sigma_{\theta y} = \frac{\mu}{r}\frac{\partial\left(v_1^{R*} + v_2^{R*}\right)}{\partial\theta} = 0, \quad \text{at } \theta_1 = \pm\frac{\pi}{2}, \text{ and } r_1 > a,$$

$$\sigma_{ry} = \mu\frac{\partial\left(v_1^{R*} + v_2^{R*}\right)}{\partial r_1} = 0, \quad \text{at } |\theta_1| < \frac{\pi}{2} \text{ and } r_1 = a,$$

$$v^{i+r} + v_1^R + v_2^R = \Delta = 1, \quad \text{at } r_2 = b. \tag{26}$$

Compared with the derivation in Section 2.2, the unknown coefficients $A_n^*$, $B_n^*$, $C_n^*$, and $D_n^*$ can be obtained by solving the linear equations (12)~(17) and (22) but removing the terms that correspond to the free-field. After that, the foundation impedance function $K_{yy}$ can be obtained by integrating the stress on the foundation boundary.

$$K_{yy} = \mu b\pi k\left[C_0^* \cdot H_1^{(2)}(ka) + J_1(ka) \cdot \frac{\varepsilon_0}{2} \cdot G_{1,n}\right]. \tag{27}$$

After the normalization by the shear modulus of the half-space, the foundation impedance function $K_{yy}$ can be further written as follows:

$$\frac{K_{yy}}{\left(\beta^2\rho\right)} = k_{yy} + i \cdot \left(\frac{\omega a}{\beta}\right) \cdot c_{yy}, \tag{28}$$

where $k_{yy}$ and $c_{yy}$ are the dimensionless stiffness and radiation damping coefficients.

## 3. Method Verification

*3.1. Dimensionless Parameters.* The results in this paper can be seen as functions of the governing dimensionless parameters, which are expressed in terms of the characteristic length of the problem, $a$, and reference wave velocity, $\beta$. The dimensionless frequency $\eta$ is defined as [27]

$$\eta = \frac{2a}{\lambda} = \frac{\omega a}{\pi\beta}, \tag{29}$$

where $2a$ is canyon width and $\lambda$ is the wavelength of the shear waves in the half-space. Further, based on [28], the dimensionless parameter $\varepsilon$ which describes the relative flexibility of the shear wall to surrounding soil is defined as

$$\varepsilon = \frac{\beta H}{\beta_b b} = \frac{k_b H}{kb}. \tag{30}$$

The dimensionless parameter $\varepsilon$ has values $0 \le \varepsilon < \infty$. For a given $\varepsilon$, the first-order vibration frequency of the shear wall is at $\eta_{b1} = 1/(2\varepsilon)$. For a very stiff structure and/or very soft soil, $\varepsilon = 0$ (corresponding to a rigid shear wall added as a rigid mass to the foundation), and for a very flexible structure and/or rigid soil, $\varepsilon \longrightarrow \infty$.

Other dimensionless parameters used in this paper are the dimensionless distance between the structure and the canyon, $D/a$, and the ratios, $M_b/M_0$ and $M_0/M_S$, where $M_S$ is the mass of the soil per unit length in the $y$-direction that has been replaced by the foundation.

*3.2. Verification.* To show the verification of our solution, we set the canyon radius $a$ equal to the foundation radius $b$ and the dimensionless distance between the canyon and the foundation $D/a$ tends to be infinite, to verify whether our results of the river-side building and the canyon are consistent with the published results that correspond to single building [1] and single canyon [2].

Figures 3 and 4 show the comparison between our results and the published results when $D/a \longrightarrow \infty$. The figures

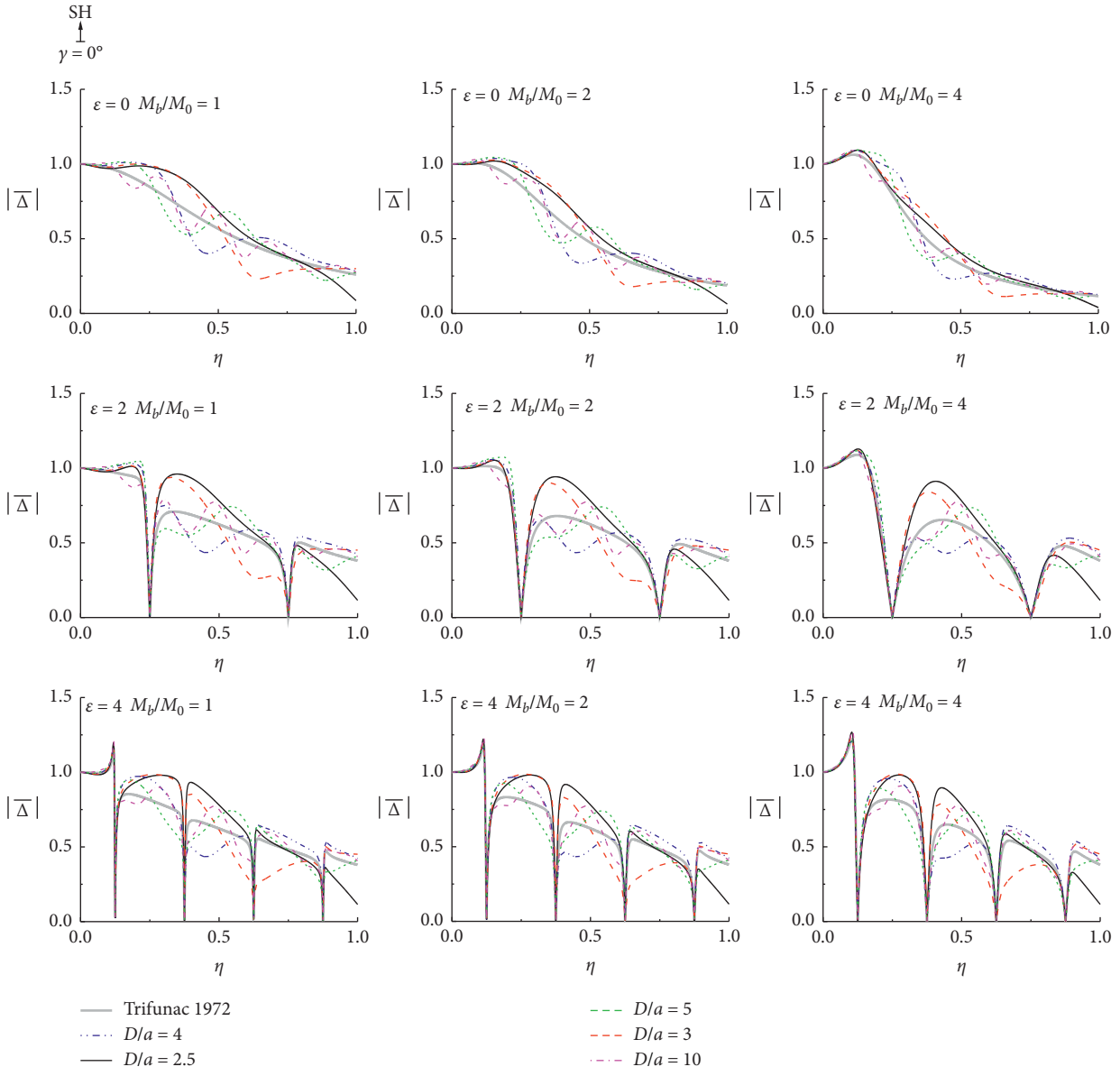


(a)

Figure 6: Continued.

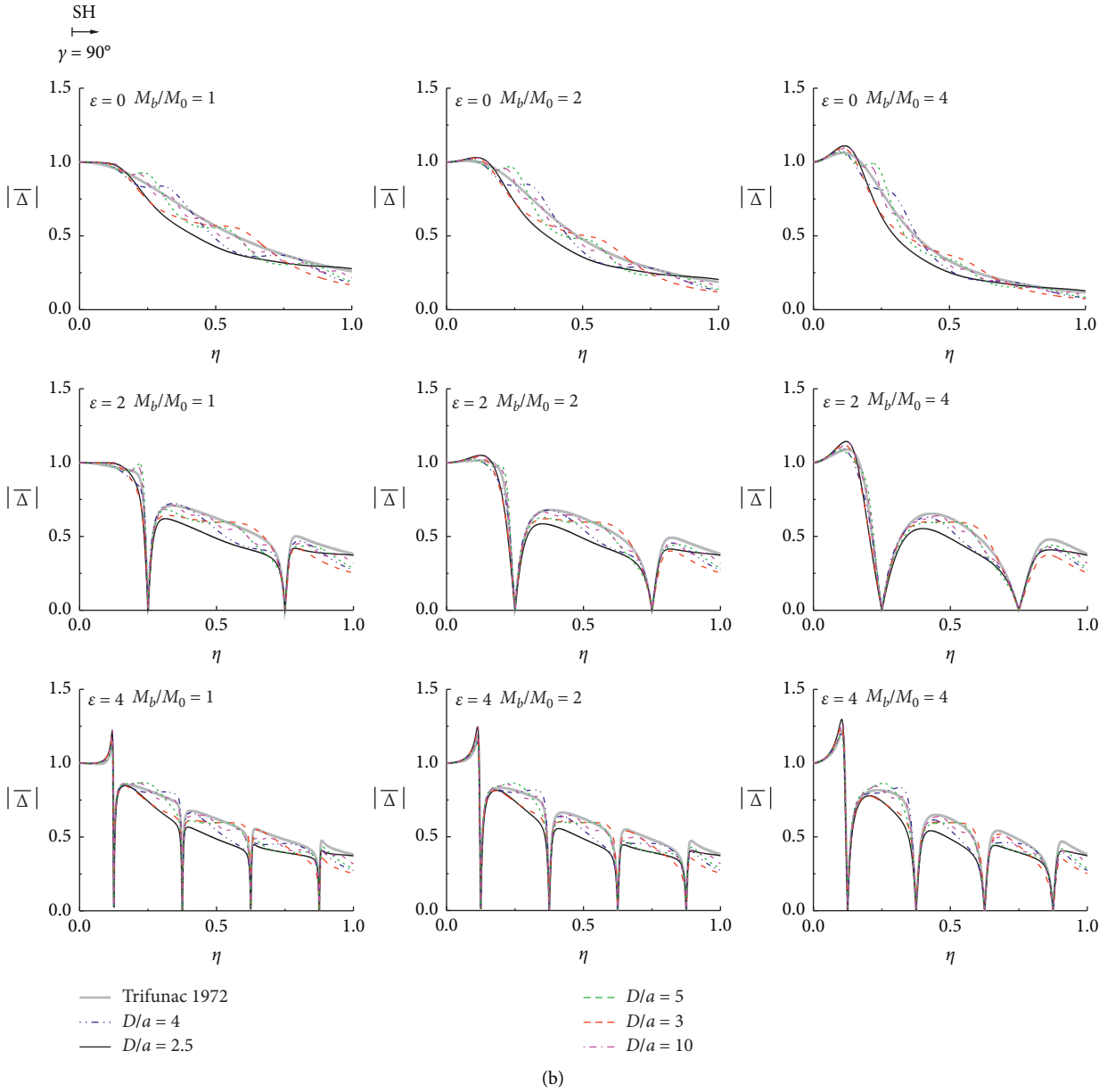


Figure 6: Foundation responses under different canyon-structure spacing. (a) Vertical incident ($\gamma = 0^{\circ}$). (b) Horizontal incident ($\gamma = 90^{\circ}$). In each part, different rows correspond to different structural stiffness $\varepsilon = 0$, 2, and 4; different columns correspond to different structural mass $M_0/M_b = 1$, 2, and 4. The mass ratio is $M_0/M_S = 1/2$.

demonstrate that our results agree well with the published results, indicating the verification of our solution.

## 4. Numerical Results and Analysis

*4.1. Model Parameters.* Figures 5–10, respectively, show foundation impedance function, foundation responses, the shear wall's relative response, and the canyon response, at different canyon-structure spacing. For easy comparison with the published results, the responses of single structure [1] and single river-canyon [2] are also shown in each subfigure. The parameters used in this section are as follows. The radius of the canyon is equal to the foundation radius; that is, $a = b$. The dimensionless distance $D/a$ between the canyon and the river-side building (referred to as "canyon-structure spacing" for short) $D/a = 2.5$, 3, 4, 5, and 10. The ratios of the foundation mass densities to the half-space mass density are 1/2, which are equivalent to $M_0/M_S = 1/2$. The mass ratio of the shear wall to the foundation per unit length is $M_b/M_0 = 1$, 2, and 4. The stiffness parameters of the shear walls are $\varepsilon = 0$, 2, and 4. The incident angles of the waves are $\gamma = 0^{\circ}$ (vertical incident) and 90° (horizontal incident).

*4.2. Foundation Impedance Function.* As shown in Figure 5, the stiffness coefficient $k_{yy}$ and damping coefficient $c_{yy}$ of the foundation impedance function are highly related to the

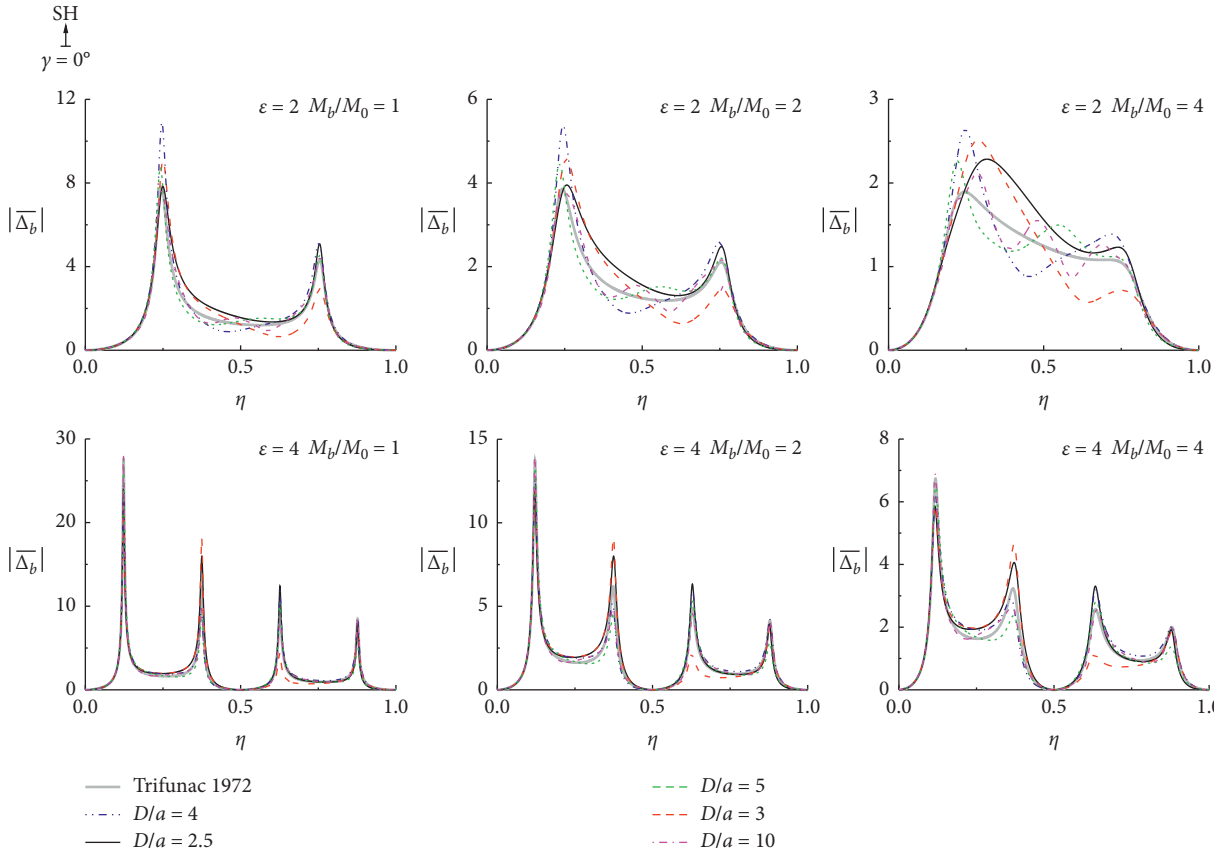


(a)

Figure 7: Continued.

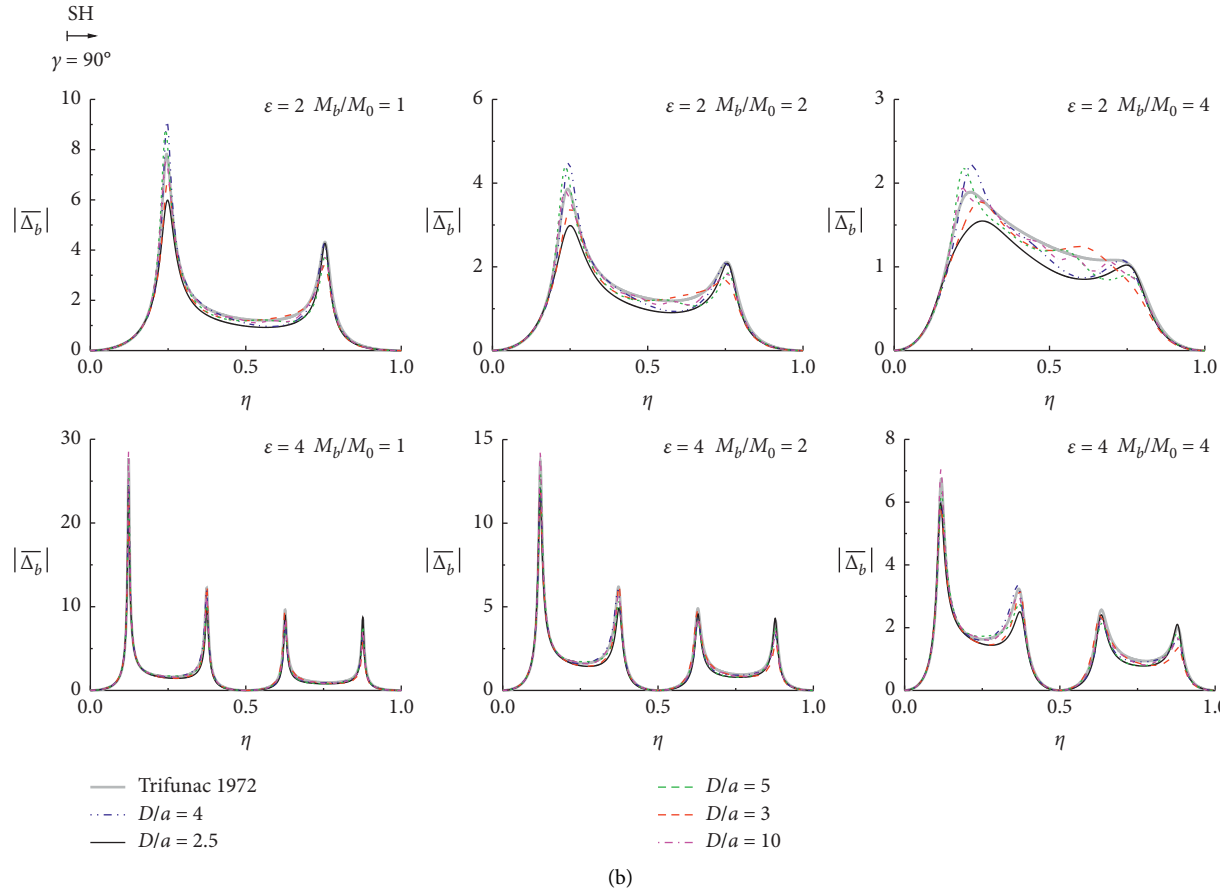


FIGURE 7: Structure relative responses to the foundation under different canyon-structure spacing. (a) Vertical incident ($\gamma = 0^{\circ}$). (b) Horizontal incident ($\gamma = 90^{\circ}$). In each part, different rows correspond to different structural stiffness $\varepsilon = 2$ and 4; different columns correspond to different structural mass $M_0/M_b = 1$, 2, and 4. The mass ratio is $M_0/M_S = 1/2$. Since structural stiffness $\varepsilon = 0$ corresponds to the case of rigid shear wall with no relative response to the foundation, the shear wall relative response related to the case of $\varepsilon = 0$ is omitted.

canyon-structure spacing ($D/a$) and the frequency of the incident wave ($\eta$). First, the stiffness coefficient $k_{yy}$ of the foundation impedance function will fluctuate strongly with different canyon-structure spacing and the frequency of the incident wave. For the closer distance between the canyon and the structure ($D/a = 2.5$, 3, 4, and 5), as the frequency of the incident wave increases, the stiffness coefficient $k_{yy}$ changes more widely. The change in the damping coefficient of the foundation impedance function is similar to the stiffness coefficient $k_{yy}$. When the frequency of the incident wave is small, the damping coefficient $c_{yy}$ is roughly the same as that of the single rigid foundation [29]. As the frequency of the incident wave increases, the damping coefficient $c_{yy}$ will also fluctuate around the damping coefficient of the single rigid foundation impedance function ($D/a \longrightarrow \infty$). However, the amplitude of the fluctuation of the damping coefficient $c_{yy}$ is smaller than that of the stiffness coefficient $k_{yy}$.

*4.3. Building Responses for Different Canyon-Structure Spacing.* Figure 6 shows how the foundation response varies with the canyon-structure spacing ($D/a$) under different incident angles ($\gamma$). Observing Figure 6, we can see that, under different canyon-structure spacing, the difference between the peak of foundation response and the peak of single foundation response is small. This can be explained as follows. First, when the frequency of the incident wave is small, the wavelength of the wave is longer, resulting in strong wave diffraction. Therefore, even if the foundation is close to the canyon, the incident wave cannot feel well the existence of the canyon due to wave diffraction, which leads to a weak interaction between the canyon and the foundation. The foundation vibrates like a single foundation, so the peak of the foundation response has a small difference from that of the single foundation. Secondly, when the distance between the canyon and the structure is large, the system interaction is also naturally weaker. From this, the two factors that determine the strength of the interaction between the canyon and the foundation can be known: the canyon-structure spacing and the wavelength of the incident wave (that is, the frequency of the incident wave). The proof for this is as follows: for example, when $\eta = 0.5$, the wavelength of the incident wave is $\lambda = 4a$. For canyon-structure spacing $D/a = 2.5$, 3, 4, and 5, the wavelength is the same order of magnitude and close to the canyon-structure

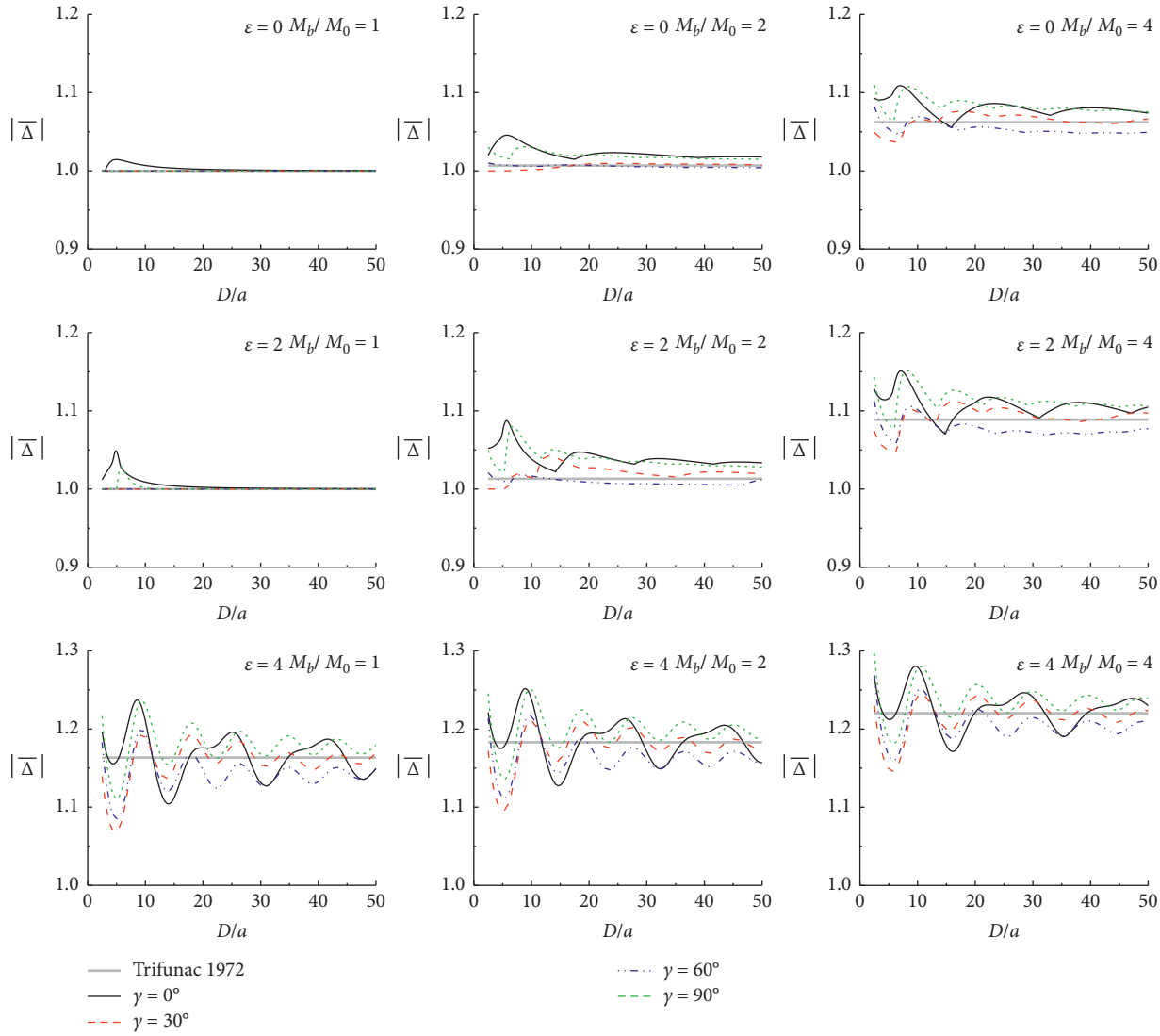


FIGURE 8: Peaks of foundation responses under different canyon-structure spacing and incident angles. Structural stiffness $\varepsilon = 0$, 2, and 4 corresponding to different rows, respectively. Different columns correspond to different $M_0/M_b = 1$, 2, and 4. The ratios are $D/a = 2.5 - 50$ and $M_0/M_S = 1/2$.

spacing. Therefore, foundation response corresponding to these locations under $\eta = 0.5$ deviates significantly from that of the single rigid foundation.

It can be seen from Figure 7 that the canyon-structure interaction has a great influence on the peak of structure relative response, which is mainly reflected in the case of structural stiffness $\varepsilon = 2$. As shown in Figure 7(a), when $\varepsilon = 2$ and $D/a$, for different superstructure masses $M_b/M_0 = 1$, 2, and 4, the peaks of the structure relative responses are 10.910, 5.377, and 2.648, respectively, while the corresponding peaks of the single structure relative response are 7.825, 3.857, and 1.893, respectively, which are enlarged by 39.4%, 39.4%, and 39.9%, respectively. Besides, observing the results under different incident angles ($\gamma$), it can be found that when the wave is incident obliquely ($\gamma = 90^\circ$), the peak of the structure relative response has a small difference from the corresponding result of the single building. However, when the wave is incident perpendicularly ($\gamma = 0^\circ$), the difference is large. The influence of the canyon-structure interaction on the structure relative response is mainly reflected in the case of vertical incidence. It can be concluded from this that another factor that determines the strength of the interaction between the canyon and the river-side building is the incident angle of the wave. The influence of the incident angle ($\gamma$) on the system interaction cannot be ignored. The deviation magnitude of the foundation response in Figure 6 and the structure relative response in Figure 7 from the single foundation result under the horizontal incidence are significantly smaller than those of the vertical incidence of the wave. This phenomenon can be called the "shielding effect." In other words, when the wave is incident obliquely, the left canyon has the effect of shielding the incident wave reaching the foundation, leading to weak foundation response and structure relative response.

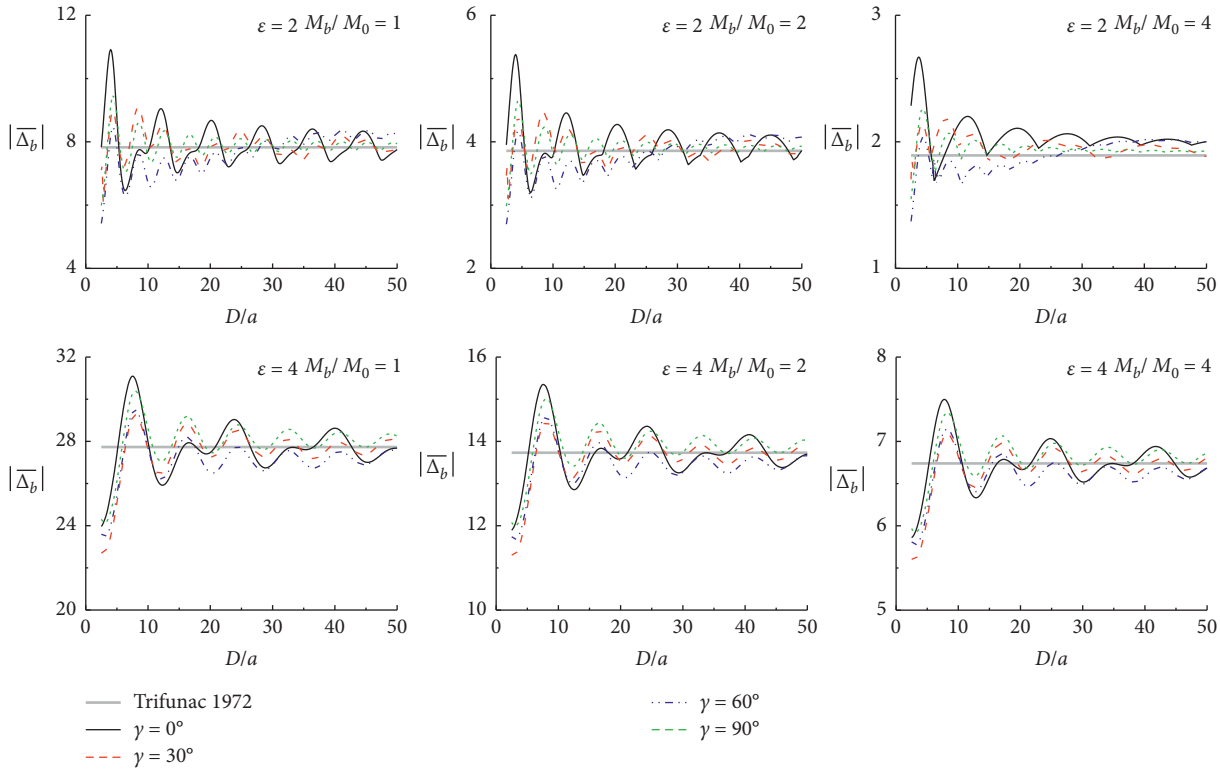


Figure 9: Same as Figure 8 but for the peaks of shear walls' relative responses.

*4.4. Peak of Structure Relative Response under Different Canyon-Structure Spacing.* Figures 8 and 9, respectively, show the variation of the foundation peak response and the shear wall's peak relative response with the canyon-structure spacing ($D/a$). As shown in Figures 8 and 9, both the foundation peak response and the shear wall's peak relative response show an attenuation trend as the canyon-structure spacing increases, but the foundation peak response and the shear wall's peak relative response are always greater than those results of single building model [1] ( the gray line in Figures 8 and 9). This phenomenon is still obvious even when the distance between the canyon and the structure is very large ($D/a = 40$~$50$). This illustrates that even when the canyon and the structure are far away, there still is an obvious interaction between them. The peak of the foundation response can be enlarged by approximately 10% (corresponding results of $\varepsilon = 2$ and $M_0/M_b = 2$ in Figure 8), and the peak of the shear wall's relative response can be amplified by approximately 39.4% (corresponding results of $\varepsilon = 2$ and $M_0/M_b = 1$ and 2 in Figure 9).

The degree to which the color line deviates from the gray line in Figure 9 can be regarded as the degree of interaction between the river-canyon and the building. It can be seen from Figure 9 that the strength of the interaction between the river-canyon topography and the building changes periodically as the distance between the canyon and the structure increases, leading to the interaction having beneficial or harmful effects on the building's seismic response. In many valley-structure intervals, the results of the valley-structure interaction model are greater than the results of single building model [1]. The distribution of valley-structure spacing with strong or weak interaction is closely related to the dynamic characteristics of the building itself and the incident angle of the wave. Therefore, when designing buildings along the river, the building and canyon should be modeled and analyzed as a whole to determine whether the location of the building is in a position with strong interaction with the river-canyon.

*4.5. Canyon Response.* Figure 10 shows the responses of canyon observation points under different incident angles and canyon-structure spacing. When the waves are vertical incident, because point 5 of the canyon is the closest to the building, the response of point 5 is the strongest, especially when the building is close to the river ($D/a = 2.5$, 3, 4, and 5). When the wave is incident obliquely, since point 1 is on the side of the incoming wave, the response of point 1 becomes the strongest, while the dynamic response at point 5 is less than that at point 1 because the river-canyon shields the wave.

Another important phenomenon is that canyon response is affected by the dynamic characteristics of the buildings, especially for small canyon-structure spacing ($D/a = \leq 5$). For example, the response of point 5 becomes zero at the fundamental frequency of the building. This phenomenon is very similar to the foundation response; that is, at the fundamental frequency of the building, the

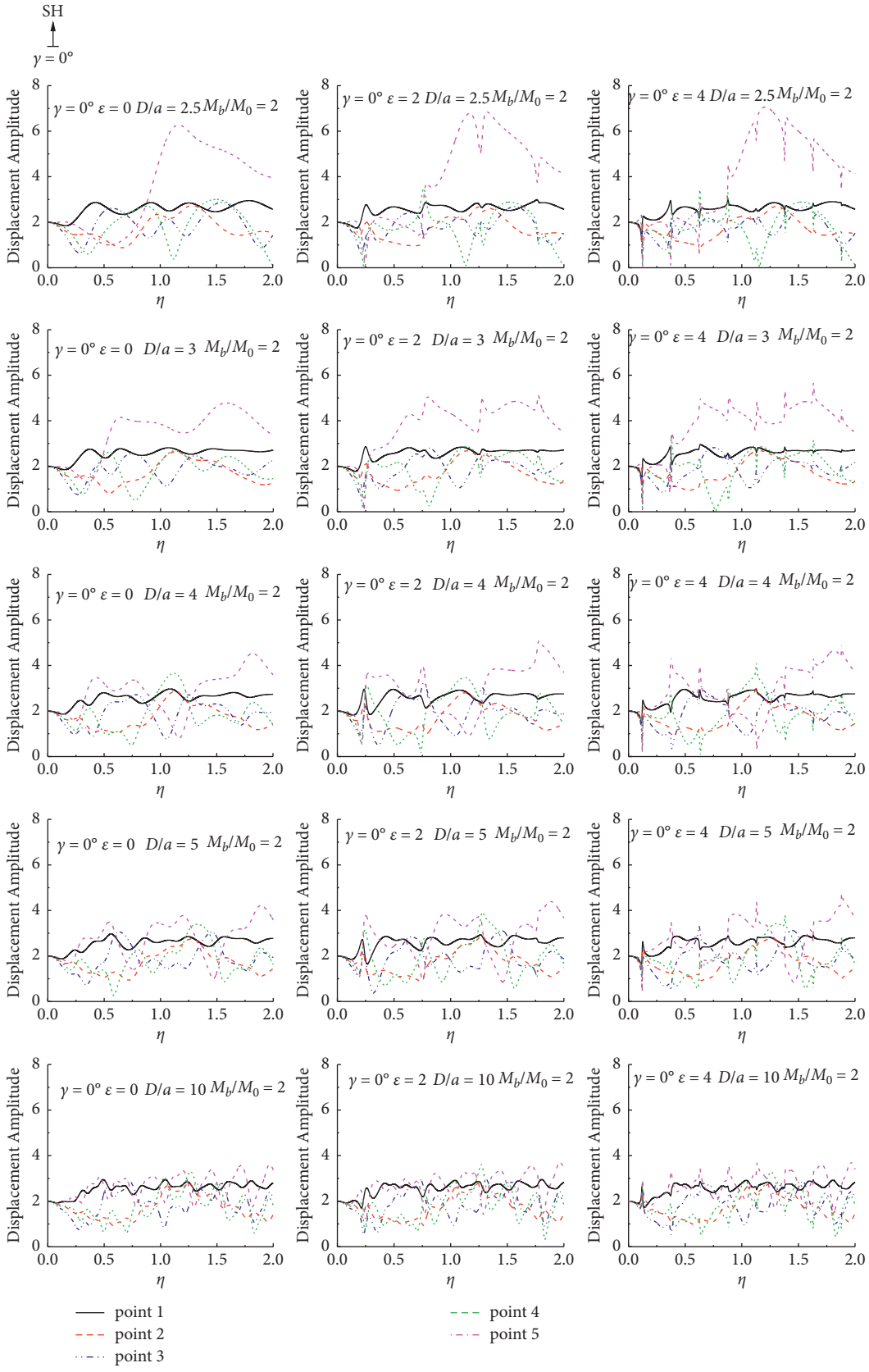


(a)

Figure 10: Continued.

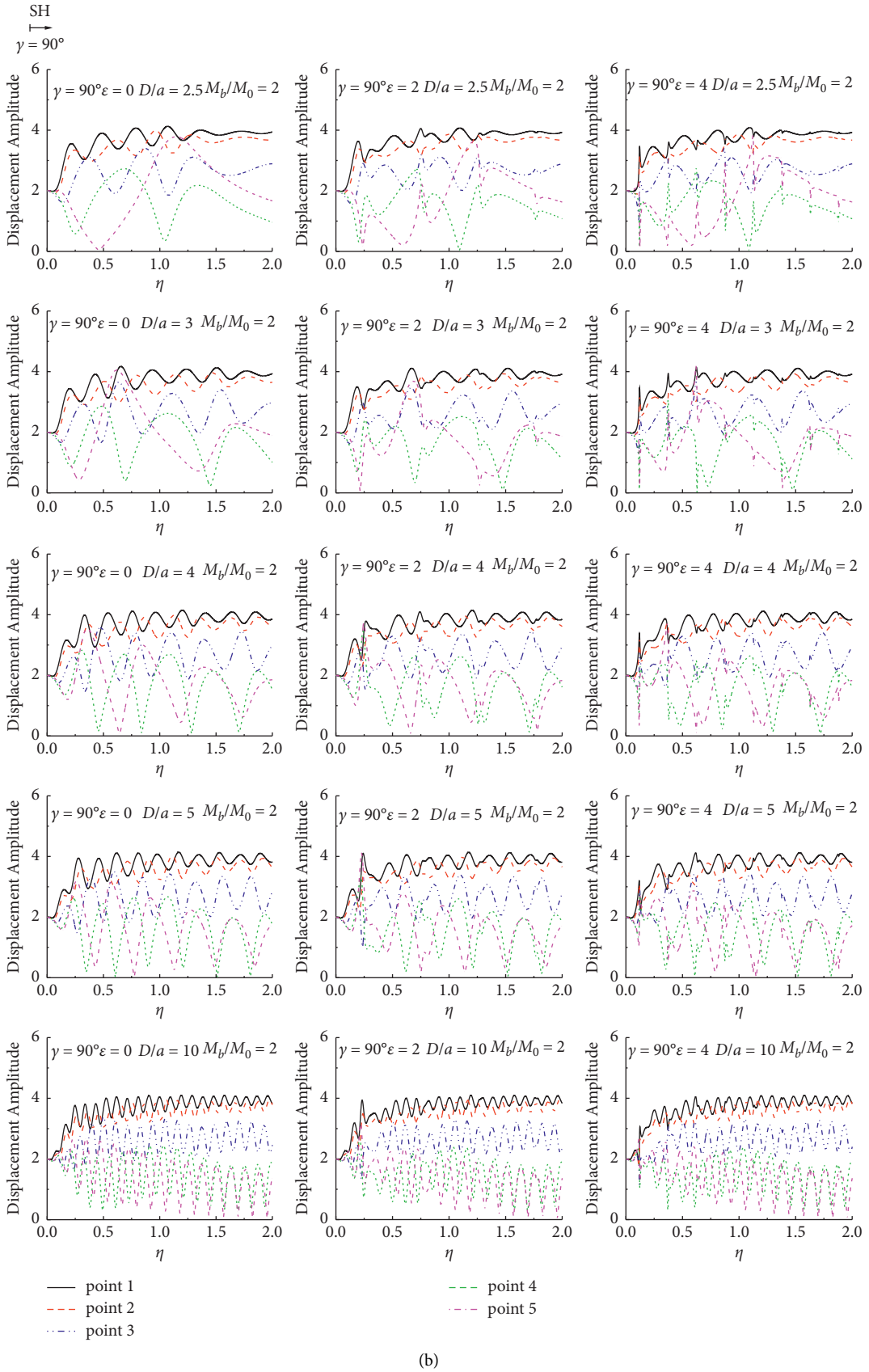


(b)

FIGURE 10: Typical spectral amplification of the canyon under different canyon-structure spacing and incident angles. Structural stiffness $\varepsilon = 0$, 2, and 4. The mass ratios are $M_0/M_b = 2$ and $M_0/M_S$.

foundation response tends to be zero. As mentioned in Section 3.1, for given $\varepsilon$, the first-order vibration of the structure is at $\eta_{b1} = 1/(2\varepsilon)$. In Figure 10, since the structural stiffness parameters are $\varepsilon = 4$, the first-order vibration frequency of the building is $\eta_{b1} = 0.125$. It can be seen from Figure 10 that, for $D/a = <5$ and $\eta = 0.125$, the response of point 5 tends to be zero. Even when the buildings are all far from the canyon ($D/a = 10$), this trend can still be observed.

## 5. Conclusions

This paper established a 2D model for the anti-plane dynamic interaction between the urban river-canyon and the river-side building and presented a closed-form analytical solution for the system response based on the wave function expansion method. The main features of the interaction between the river-canyon and the building along the river are investigated by the analytical solution. The conclusions and findings are as follows:

(1) The canyon-structure interaction depends not only on the distances between the canyon and the river-side building but also on the frequency of the incident wave and the incident angle. When the wave is incident obliquely, the canyon on the incoming wave side has the shielding effect on the incident wave.

(2) The strength of the interaction between the river-canyon topography and the building changes periodically as the distance between the canyon and the structure increases, leading to the interaction having beneficial or harmful effects on the building's seismic response. The results in this paper show that the foundation peak response of the building can be amplified by about 10%, and the peak of the building relative response can be amplified by about 40%.

(3) The distribution of valley-structure spacing with strong or weak interaction is closely related to the dynamic characteristics of the building and the incident angle of the wave. When designing buildings along the river, the building and canyon should be modeled and analyzed as a whole to determine whether the location of the building is in a position with strong interaction with the river-canyon.

(4) The canyon response of the canyon is closely related to the frequency of the incident wave, the canyon-structure spacing, the incident angle of the wave, and the dynamic characteristics of the building along the river.

## Data Availability

The data used to support the findings of this study are available from the corresponding author upon request.

## Conflicts of Interest

The authors declare that the work is original research that has not been published previously, and not under consideration for publication elsewhere. No conflicts of interest exist in the submission of this paper.

## Authors' Contributions

This study was approved by all authors for publication.

## Acknowledgments

This study was supported by the National Natural Science Foundation of China under Grants 51808290 and U1839202, which are gratefully acknowledged.

## References

[1] M. D. Trifunac, "Dynamic interaction of a shear wall with the soil for incident plane SH Waves," *Bulletin of the Seismological Society of America*, vol. 62, pp. 62–83, 1972.

[2] M. D. Trifunac, "Scattering of plane SH waves by a semi-cylindrical canyon," *Earthquake Engineering & Structural Dynamics*, vol. 1, pp. 267–281, 1973.

[3] P. Guéguen, P. Y. Bard, and F. J. G. Chávez, "Site-city seismic interaction in Mexico city-like environments: an analytical study," *Bulletin of the Seismological Society of America*, vol. 92, no. 2, pp. 794–811, 2002.

[4] M. Kham, J. F. Semblat, P. Y. Bard, and P. Dangla, "Seismic site-city interaction: main governing phenomena through simplified numerical models," *Bulletin of the Seismological Society of America*, vol. 96, no. 5, pp. 1934–1951, 2006.

[5] P. Y. Bard, J. L. Chazelas, P. Guéguen, M. Kham, and J. F. Semblat, "Site-city interaction," in *Assessing and Managing Earthquake Risk*, pp. 91–114, Springer, Netherlands, 2008.

[6] H. L. Wong and P. C. Jennings, "Effects of canyon topography on strong ground motion," *Bulletin of the Seismological Society of America*, vol. 65, pp. 1239–1259, 1975.

[7] H. L. Wong, "Effect of surface topography on the diffraction of P, SV and Rayleigh waves," *Bulletin of the Seismological Society of America*, vol. 72, no. 4, pp. 1167–1183, 1982.

[8] D. H. Tsaur and K. H. Chang, "Scattering of SH waves by truncated semicircular canyon," *Journal of Engineering Mechanics*, vol. 135, no. 8, pp. 862–870, 2009.

[9] G. D. Manolis and P. S. Dineva, "Elastic waves in continuous and discontinuous geological media by boundary integral equation methods: a review," *Soil Dynamics and Earthquake Engineering*, vol. 70, pp. 11–29, 2015.

[10] N. Zhang, Y. Zhang, Y. Gao, R. Y. S. Pak, and J. Yang, "Site amplification effects of a radially multi-layered semi-cylindrical canyon on seismic response of an earth and rockfill dam," *Soil Dynamics and Earthquake Engineering*, vol. 116, pp. 145–163, 2019.

[11] V. W. Lee and H. Cao, "Diffraction of SV waves by circular canyons of various depths," *Journal of Engineering Mechanics*, vol. 115, no. 9, pp. 2035–2056, 1989.

[12] H. Cao and V. W. Lee, "Scattering and differaction of plane P waves by circular cylindrical canyons with variable depth-to-width ratio," *Soil Dynamics and Earthquake Engineering*, vol. 9, no. 3, pp. 141–150, 1990.

[13] J. W. Liang, L. J. Yan, J. W. Li, and V. W. Lee, "Response of circular-arc alluvial valleys under incident plane P waves," *Rock and Soil Mechanics*, vol. 22, no. 2, pp. 138–143, 2001.

[14] J. W. Liang, L. J. Yan, and V. W. Lee, "Scattering of plane P waves by circular-arc layered alluvial valleys: an analytical

solution," *Acta Seismologica Sinica (Chinese edition)*, vol. 23, no. 2, pp. 167–184, 2001.

[15] N. Zhang, Y. Gao, Y. Cai, D. Li, and Y. Wu, "Scattering of SH waves induced by a non-symmetrical V-shaped canyon," *Geophysical Journal International*, vol. 191, no. 1, pp. 243–256, 2012.

[16] N. Zhang, Y. Gao, D. Li, Y. Wu, and F. Zhang, "Scattering of SH waves induced by a symmetrical V-shaped canyon: a unified analytical solution," *Earthquake Engineering and Engineering Vibration*, vol. 11, no. 4, pp. 445–460, 2012.

[17] Y. Gao and N. Zhang, "Scattering of cylindrical SH waves induced by a symmetrical V-shaped canyon: near-source topographic effects," *Geophysical Journal International*, vol. 193, no. 2, pp. 874–885, 2013.

[18] Y. Gao, N. Zhang, D. Li, H. Liu, Y. Cai, and Y. Wu, "Effects of topographic amplification induced by a U-shaped canyon on seismic waves," *Bulletin of the Seismological Society of America*, vol. 102, no. 4, pp. 1748–1763, 2012.

[19] N. Zhang, Y. Zhang, Y. Gao, R. Y. S. Pak, Y. Wu, and F. Zhang, "An exact solution forSH-wave scattering by a radially multilayered inhomogeneous semicylindrical canyon," *Geophysical Journal International*, vol. 217, no. 2, pp. 1232–1260, 2019.

[20] V. W. Lee and J. Karl, "Diffraction of SV waves by underground, circular, cylindrical cavities," *Soil Dynamics and Earthquake Engineering*, vol. 11, no. 8, pp. 445–456, 1992.

[21] V. W. Lee and J. Karl, "On deformations of near a circular underground cavity subjected to incident plane P waves," *European Journal of Engineering Education*, vol. 1, pp. 29–36, 1993.

[22] K. Zhao, Q. Wang, Q. Chen, H. Zhuang, and G. Chen, "Simplified effective stress simulation of shear wave propagation in saturated granular soils," *Géotechnique Letters*, vol. 11, no. 1, pp. 1–22, 2021.

[23] L. Y. Xu, C. X. Song, W. Y. Chen, F. Cai, Y. Y. Li, and G. X. Chen, "Liquefaction-induced settlement of the pile group under vertical and horizontal ground motions," *Soil Dynamics and Earthquake Engineering*, vol. 144, Article ID 106709, 2021.

[24] C. Liu, J. Cui, Z. Zhang, H. Liu, X. Huang, and C. Zhang, "The role of TBM asymmetric tail-grouting on surface settlement in coarse-grained soils of urban area: field tests and FEA modelling," *Tunnelling and Underground Space Technology*, vol. 111, Article ID 103857, 2021.

[25] M. Abramowitz and I. A. Stegun, *Handbook of Mathematical Functions with Formulas, Graphs, and Mathematical Tables*, Dover, NY, USA, 1972.

[26] L. Jin and J. Liang, "Dynamic soil-structure interaction with a flexible foundation embedded in a half-space: closed-form analytical solution for incident plane SH waves," *Journal of Earthquake Engineering*, vol. 25, no. 8, pp. 1565–1589, 2021.

[27] M. I. Todorovska and M. D. Trifunac, "The system damping, the system frequency and the system response peak amplitudes during in-plane building-soil interaction," *Earthquake Engineering & Structural Dynamics*, vol. 21, no. 2, pp. 127–144, 1992.

[28] J. Liang, J. Fu, M. I. Todorovska, and M. D. Trifunac, "Effects of the site dynamic characteristics on soil-structure interaction (I): incident SH-waves," *Soil Dynamics and Earthquake Engineering*, vol. 44, pp. 27–37, 2013.

[29] F. C. P. D. Barros and J. E. Luco, "Dynamic response of a two-dimensional semi-circular foundation embedded in a layered viscoelastic half-space," *Soil Dynamics and Earthquake Engineering*, vol. 14, no. 1, pp. 45–57, 1995.